



Valorization of *Inula viscosa* waste extraction, modeling of isotherm, and kinetic for the tartrazine dye adsorption

M. Kebir^{a,b,c,*}, M. Trari^a, R. Maachi^b, N. Nasrallah^b, A. Amrane^{d,e}

^aFaculty of Chemistry, Laboratory of Storage and Valorization of Renewable Energies, USTHB, BP 32, Algiers, Algeria, Email: medkbeir@yahoo.fr

^bFaculty of Mechanical Engineering and Process Engineering, Laboratory of Reaction Engineering, USTHB, BP 32, Algiers, Algeria

^cTechnical and Scientific Research Centre of Physico-Chemicals Analysis (CRAPC), BP 248, RP 16004 Algiers, Algeria

^dEcole Nationale Supérieure de Chimie de Rennes, CNRS, UMR 6226, Université de Rennes 1, Avenue du Général Leclerc, CS 50837, 35708 Rennes Cedex 7, France

^eUniversité européenne de Bretagne, Rennes, France

Received 5 November 2013; Accepted 27 February 2014

ABSTRACT

The aim of this study was the tartrazine dye removal from aqueous solutions using a solid waste from the essential oil extraction of *Inula viscosa*. Experiments carried out in batch mode showed that the adsorption depended on physical parameters such as pH, adsorbent dose, initial pollutant concentration, and temperature. The results of scanning electron microscopy and energy dispersion X-ray indicated that the potential to adsorb tartrazine dye onto *I. viscosa* was related to the adsorbent structure. The nature of the surface groups on the adsorbent was determined from the Fourier transform infrared spectroscopy and specific surface area. The dye retention was found to be pH-dependent and the tartrazine adsorption decreased with increasing pH over the pH range (1–6). The Langmuir, Freundlich, Temkin, and Dubinin–Radushkevich isotherm models were used to analyze the adsorption behavior. The maximum adsorption capacity was found to be $\sim 43.1 \text{ mg g}^{-1}$ at pH 2 and 298 K. Dye adsorption kinetic was well described by a pseudo-second-order model. The thermodynamic parameters indicated that the adsorption of tartrazine was spontaneous and endothermic, and the process was governed by physisorption owing to the low enthalpy. Therefore, *I. viscosa* is promising as a low-cost adsorbent for the dye removal from aqueous solutions.

Keywords: Adsorption; Tartrazine; Isotherm; Kinetic; Thermodynamic parameters

1. Introduction

Industrial processes produce large volumes of polluted effluents which are released in the aquatic environment without any treatment. The dyes are used in several industries like the textile, pulp, leather, dyes

synthesis, printing, food, soft drinks, and plastics to improve the appearance and natural color [1]. Tartrazine (E102) is used in the food industry and in presence of other compounds forms complex molecular structures harmful to the environment and humans. It causes allergies, skin irritation, childhood, asthma, mutation in humans, and itching. It also has toxic effects on the human corneal epithelium [2]. These

*Corresponding author.

complex structures act as catalysts of the hyperactivity and other behavioral problems when they are discharged into the aquatic medium [3,4]. Indeed, the tartrazine is a nitrous derivative known to cause allergic reactions and has been the focus of studies on mutagenesis and carcinogenesis due to its transformation into aromatic amine sulfanilic acid after being metabolized by the gastrointestinal microflora [5].

Algeria is home of several wild medicinal plants among which is *Inula viscosa*. This plant has received an increased interest in both pharmaceutical and food industries. The extraction process generates aqueous oil along with a solid waste residue. The latter is a pollutant for the environment and its disposal in landfills must be avoided. The objectives of this study are twofold, on the one hand, the management of the solid waste discharged into the environment, and on the other hand, its re-utilization as adsorbent for pollutants removal to reduce the risk of water pollution [6]. Despite these fruitful attempts, the development of this low-cost material represents an attractive alternative with respect to conventional waste treatments like the biodegradation, the photocatalytic degradation, the ion exchange, membranes, coagulation–flocculation, and adsorption [5,7–11]. In comparison to all these techniques, the adsorption is becoming a potential treatment for the dyes removal [11] and has found to have large-scale applications. It is clean, easy to handle, low cost [12], and has high pollutant removal because of its cost, robustness, and environmentally friendly characteristics [13].

In this respect, the activated carbon is currently used for the wastewaters treatment. However, given the high cost associated with its preparation, many investigators have studied the feasibility of cheaper materials as possible replacements for the pollution abatement treatment [6,14,15]. Activated carbon plays a significant role in the environmental protection and prevention of global warming and reduces the pollution level below the detection threshold. In this respect, extensive works have been focused on the tartrazine removal on different adsorbents such as bottom ash, de-oiled Soya [16], hen feathers [17], and chitin products [18]. However to the authors' knowledge, no study has previously been done for tartrazine removal onto *I. viscosa*. In this paper, the solid waste produced from the essential oil extraction of *I. viscosa* is successfully used for the tartrazine removal. The operating factors including the initial pH, the contact time, the initial dye concentration, the adsorbent dosage, and the temperature are varied to determine their effects on the adsorption process. Equilibrium isotherm and kinetic studies are performed for modeling the experimental data and evaluating the adsorption

process. A thermodynamic study is also undertaken to determine the nature of the adsorption.

2. Experimental

2.1. Preparation of adsorbent

Essential oil extraction of *I. viscosa* was performed in a laboratory setup. The solid waste residue (adsorbent) produced from the extraction process was collected and thoroughly washed with distilled water to remove the dust and extraction impurities and dried in air oven. The adsorbent structure was then treated chemically by impregnation in NaOH (0.1 M) for 6 h to remove the color. To remove traces of NaOH, the adsorbent was washed several times with water and dried at 80°C overnight. Then, the dried material was crushed with a mechanical grinder and stored in a glass bottle.

The characterization of the adsorbent was carried out by means of scanning electron microscopy (SEM) using a Philips XL 30 microscope coupled with an energy dispersive X-ray spectroscopy (EDX). Samples for EDX analysis were coated with a thin carbon film in order to avoid the influence of charge effect during the SEM operation. Fourier transform infrared spectroscopy (FTIR) was used to determine the functional groups using a Spectrum 1 (Spectrum One FTIR Perkin-Elmer, Waltham, MA, USA) with a resolution of 2 cm⁻¹. Pressed KBr pellets (sample/KBr *wt.* ratio = 1:100) were placed in an oven at 120°C for 5 h to remove the moisture and subjected to a scanning range (3,400–400 cm⁻¹).

The specific surface area and pore volume were determined from nitrogen adsorption experiments at 77 K using a Quantachrome Instruments analyzer (Quantachrome Corporation, USA). The adsorbent surface charge (pH_{zc}) was determined by the solid-adding method [19]. Known amounts of activated adsorbent were suspended in 25 mL of NaCl (0.1 M) and the pH was adjusted between 2 and 10 using HCl or NaOH solutions and the mixtures were then mixed by a magnetic stirring for 48 h. pH_{zc} corresponds to no change in the pH after contact with adsorbent; the final pH_{fin} of the solution was measured with a pH-meter (Hanna Instruments HI 2210 Benchtop pH Meter, Woonsocket, RI, USA).

2.2. Adsorption study

Experiments were carried out in batch mode in a Pyrex reactor containing 500 mL of tartrazine solution and adsorbent under agitation (300 rpm). The contact time, the initial dye concentration (25–200 mg L⁻¹), the

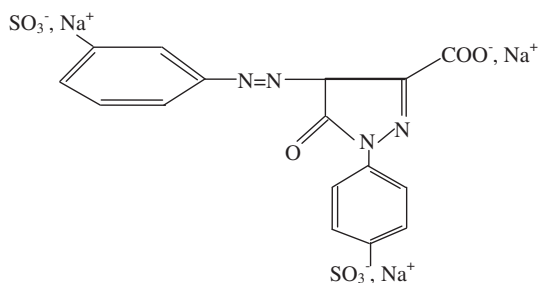


Fig. 1. Chemical structure of tartrazine dye.

initial pH (1–6), the adsorbent dose (2–6 g), and the temperature (20–50°C) were studied. The experimental protocol was performed such that for a given test, only one parameter was changed keeping the others constant. The chemical formula of tartrazine is $C_{16}H_9N_4Na_3O_9S_2$ (MW: $534.363 \text{ g mol}^{-1}$) and its structure is shown Fig. 1. The dye concentration was monitored by UV/visible spectrophotometer (UV-1800, Shimadzu, Nakagyo-ku, Kyoto, Japan) at the maximum wavelength ($\lambda_{\text{max}} = 620 \text{ nm}$) using a linear regression of the calibration curve. All measurements were carried out in triplicate and blank tests were performed. The removal efficiency ($R\%$) and the adsorption capacity (q_e) of the tartrazine onto *I. viscosa* were calculated from the concentrations (C_o), (C_t) at time (t), and equilibrium (C_e) by the following Eqs. (1) and (2), respectively:

$$R\% = \frac{100(C_o - C_t)}{C_o} \quad (1)$$

$$q_e = \frac{V(C_o - C_e)}{m} \quad (2)$$

where V is the volume of the solution (L) and m is the mass of adsorbent (g).

3. Results and discussion

3.1. Characterization of the adsorbent

The morphology of *I. viscosa* adsorbent was characterized by SEM to show the surface texture and porosity (Fig. 2(a) and (b)). Micrographs of the raw adsorbent before (Fig. 2(a)) show a porous structure with a rough heterogeneous surface. However, the micrograph after activation (Fig. 2(b)) indicates some morphological differences due to the development of new larger pores during the activation process. The elemental composition of the adsorbent was analyzed

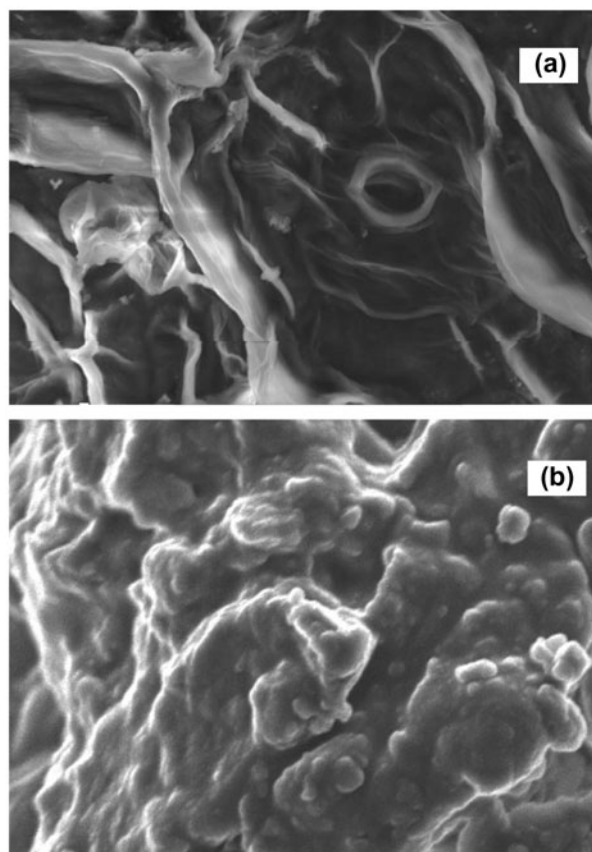
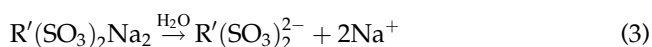


Fig. 2. Scanning electron micrographs SEM image (a) of activated *I. viscosa* (25 kV \times 1,000; 10 μm) and (b) raw *I. viscosa* (5 kV \times 10,000; 1 μm).

using SEM/EDX. EDX spectrum shows that carbon, oxygen, sodium, and calcium are the main elements of the adsorbent (Table 1), while other elements such as Si, K, and Fe are present only in small percentages.

The initial pH vs. final pH is plotted in Fig. 3. pH_{zc} corresponds to the intersection point of pH_{ini} vs. pH_{fin} indicating that the material has a zero charge at pH 5.8; at lower pHs ($<\text{pH}_{\text{zc}}$), the charge is positive and the dye removal should be high. Indeed, aqueous solution, tartrazine, ($\text{R}'(\text{SO}_3)_2\text{Na}_2$) is dissolved and the acidic sulfonate groups of the dye are dissociated and converted to anionic dye ions according to the following reaction (3):



The adsorption occurs between the anionic dye $\text{R}'(\text{SO}_3)_2^{2-}$ and the functional groups of the adsorbent. Tartrazine forms a stable ion pair when dissociated

Table 1
Chemical composition of activated *I. viscosa*

Element	Wt%
C	68.21
O	27.00
Na	01.56
Mg	00.15
Al	00.11
Si	00.09
S	00.10
K	00.07
Ca	01.87
Fe	00.04
Ni	00.11
Cu	00.42
Zn	00.29

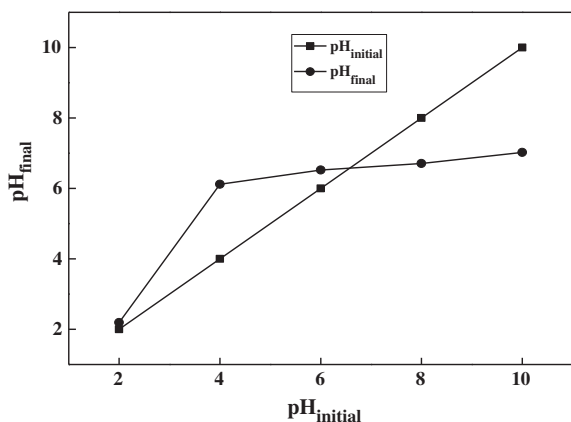


Fig. 3. Initial vs final pH plot for the determination of the pH_{zc} of *I. viscosa*.

and undergoes surface interaction with the aromatic ring of the resin which also induces physical adsorption and dispersion forces [20]. Physical and chemical properties like moisture content, bulk density, and porosity are given in Table 2.

The FTIR spectra are shown in Fig. 4. Before activation (Fig. 4(a)), the broad band located at $3,438\text{ cm}^{-1}$ is related to O–H groups. The band at $2,926\text{ cm}^{-1}$ is assigned to C–H stretching related to alkanes (CH_2) deformation and alkyl groups C–O–C stretching, respectively. The band at $2,339\text{ cm}^{-1}$ is ascribed to a $\text{C}\equiv\text{C}$ vibration while the band at $1,744\text{ cm}^{-1}$ is characteristic of the stretch vibration of C=O of carboxylic acid. The transmittance at $1,446\text{--}722\text{ cm}^{-1}$ is identical to C–H in (CH_3) deformation and in $(\text{CH}_2)_n$ groups while the band at $1,155\text{ cm}^{-1}$ corresponds to C–O of alcohol groups. Fig. 4(b) corresponds to the modified

Table 2
Physical and chemical properties of *I. viscosa*

Porosity	0.2413
Moisture content (%)	1.3436
Bulk density (Real)	1.1828
Apparent density	0.4538
Pore volume ($\text{cm}^3\text{ g}^{-1}$)	0.413
Total porosity	0.6163
pH_{zc}	6.52

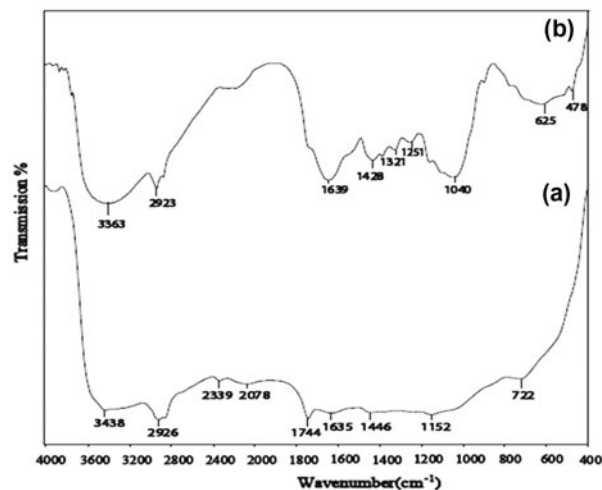


Fig. 4. FTIR spectrum of raw (a) and NaOH activated (b) *I. viscosa*.

solid residue from the *I. viscosa*; the more intense peaks of the stretching vibration at $3,363\text{ cm}^{-1}$ are assigned to O–H groups. The peak at $2,923\text{ cm}^{-1}$ can be ascribed to C–H attributed to the asymmetrical stretch vibration of $(\text{CH}_2)_2$. The strong band at $1,639\text{ cm}^{-1}$ is due to stretching vibration of C=O from carboxylic acid. The peak $1,428\text{ cm}^{-1}$ is assigned to the bending OH vibration of hydroxyl groups, while the peak of carboxylic group is shifted to $1,040\text{ cm}^{-1}$. The band at 620 cm^{-1} is related to $=\text{C}\text{--}\text{H}$ stretching or C=O bending. The FTIR analysis indicates the presence of carbonyl, hydroxyl groups on the adsorbent surface. After NaOH activation, these functional groups become intense and large. The activation includes the disappearance of some peaks ($1,744$, $2,339$ and $2,070\text{ cm}^{-1}$) and the appearance of new ones ($1,321$, $1,251$, $1,040$, 625 , and 478 cm^{-1}) due to the breaking of intermolecular bonds. It can be assumed that these surface groups are the potential active sites for the dye interaction.

The surface area (BET), Microporous area, and Micropore volume data of the samples are summarized in Table 3. It can be seen that the BET surface

area, total pore volume, mesopore volume, and average pore width were greatly improved compared to the raw adsorbent which shows that the activation treatment with NaOH do have an effect on the porosity of *I. viscosa*.

3.2. Effect of the initial pH

In the adsorption process, the pH is a crucial parameter and affects both the adsorbent surface charge and the dissociation of dye in solution. Adsorption of yellow dye tartrazine is performed with 50 mg L^{-1} initial dye concentration and over the pH range (1–6) (Fig. 5). The results obtained show that equilibrium is reached after 3 h and the high removal occurs at pH 2 with a removal percentage of 95.5%.

The effect of pH on the adsorption can be explained by considering the adsorbent charge; it should be remembered that pH_{zc} is 6.52, and hence the tartrazine exhibits a positive charge at lower pHs where at pH below pH_{zc} the electrostatic attraction between the dye and positive charge on the adsorbent surface favors the adsorption, thereby attracting the negatively charged functional groups (SO_3^-) located on the reactive dye [21]. By contrast, in alkaline solutions ($\text{pH} > \text{pH}_{\text{zc}}$), the protonation of the dye is minimized and the electrostatic repulsion between OH^- and adsorbent group and the ionized dye reduces the extent of both diffusion and adsorption [22]. Therefore, pH 2 is considered more effective and it is used for further studies.

3.3. Effect of the adsorbent dose

The adsorbent dose is another important factor which has an influence on the adsorbent capacity. The adsorption capacity (q_e) and the removal yield ($R\%$) for an initial dye concentration of 80 mg L^{-1} at various amounts of *I. viscosa* are presented in Fig. 6. With increasing the adsorbent dose from 1 to 8 g L^{-1} , the dye removal increases from 61.37 to 93%. However, the adsorption capacity shows an opposite trend, respectively, from 54.66 to 9.18 mg g^{-1} . The increase of the removal yield is mostly due to an increased specific surface area to the availability of more adsorption

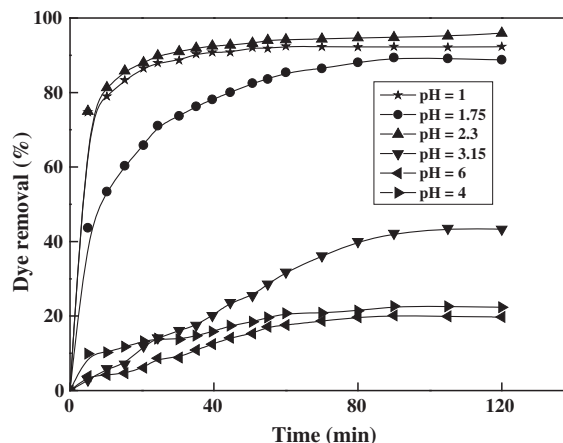


Fig. 5. Effect of pH on the tartrazine dye adsorption onto *I. viscosa* (50 mg L^{-1} , $24 \pm 2^\circ\text{C}$, 5 g L^{-1} adsorbent, 250 rpm min^{-1}).

sites and in this way and consequently to a better adsorption [23–25].

For a dose of *I. viscosa* of 5 g L^{-1} and for dye concentration of 80 mg L^{-1} , the values of q_e and $R\%$ are, respectively, 12.47 mg g^{-1} and 91.99%. Above 5 g L^{-1} , there is no significant improvement in the removal rate, while q_e decreases rapidly; this may be due to the decrease of total surface area for adsorption because of the adsorption sites aggregation. Considering q_e and $R\%$ values, adsorbent dose of 5 g L^{-1} is taken as an optimal value and is used for the remaining experiments.

3.4. Effect of the initial dye concentration and the contact time

The adsorption capacity of *I. viscosa* is greatly influenced by the initial dye concentration (C_o). A concentration range ($20\text{--}200 \text{ mg L}^{-1}$) is investigated with a fixed adsorbent amount of 5 g L^{-1} at pH 2 and 25°C . Fig. 7(b) clearly indicates an increase of the adsorbed amount with increasing C_o . At low concentrations C_o , the adsorption rate increases and saturates rapidly and the equilibrium takes place within 60 min; whereas, the high adsorption rate occurs after 120 min for high concentrations C_o . This behavior indicates that the high concentrations provide a large driving force

Table 3

Physical properties deduced from N_2 adsorption at 77 K of raw and activated *I. viscosa* with NaOH

Samples	Surface area BET ($\text{m}^2 \text{ g}^{-1}$)	Microporous area ($\text{m}^2 \text{ g}^{-1}$)	Micropore volume ($\text{cm}^3 \text{ g}^{-1}$)
Raw <i>Inula viscosa</i>	71.331	8.219	0.003
Treated <i>Inula viscosa</i>	105.188	12.485	0.546

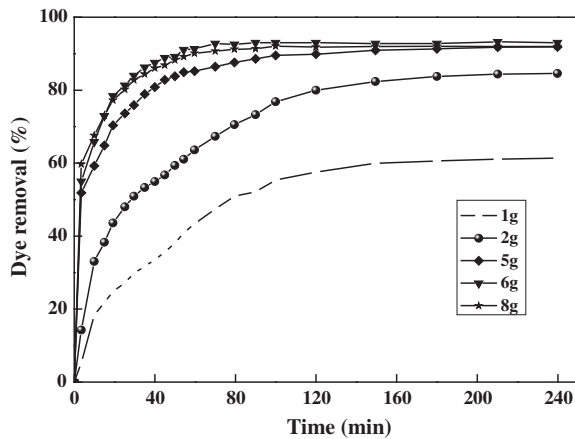


Fig. 6. Effect of the adsorbent amount on the tartrazine dye adsorption onto *I. viscosa* (50 mg L^{-1} , $24 \pm 2^\circ\text{C}$, pH 2, 250 rpm min^{-1}).

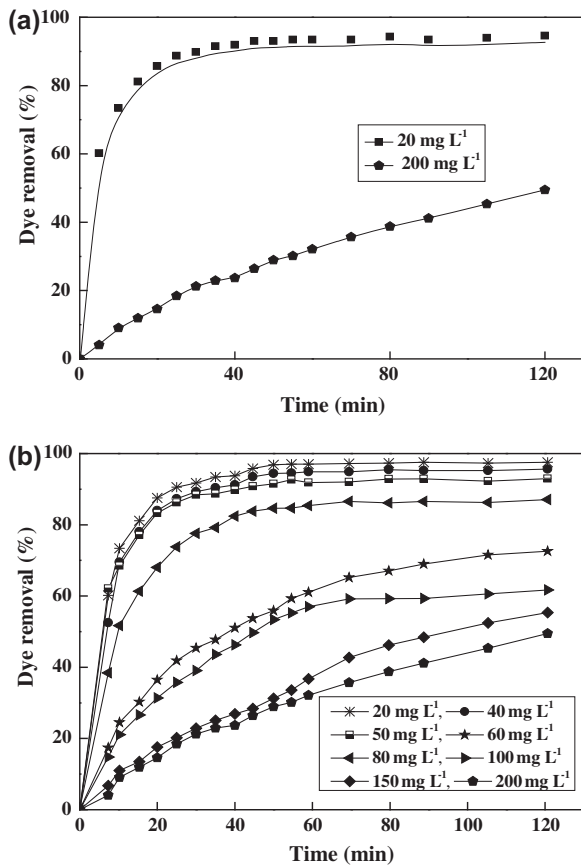


Fig. 7. Effect of the contact time (a) and the initial dye concentration (b) on dye adsorption onto *I. viscosa* ($24 \pm 2^\circ\text{C}$, pH 2, 250 rpm min^{-1} , 5 g L^{-1} adsorbent).

to overcome the mass transfer resistance of the dye on the adsorbent solid surface [26,27]. The results also show that the adsorption kinetic is divided in two

steps. The first one is rapid, due to the availability of abundant active sites that could bind the yellow dye. The second step is slow and equilibrium is reached with a constant concentration. The low increase in the dye removal should be related to the progressive occupancy of adsorbate, as well as the slow pore diffusion of the dye into the bulk of adsorbent [28]. The adsorption capacity (q_e) increases from 3.78 to 25.88 mg g^{-1} with raising C_o over the range ($20\text{--}200 \text{ mg L}^{-1}$) and this indicates that *I. viscosa* is less efficient at high concentrations C_o .

3.5. Isotherms

In order to check the adsorption capacity, the isotherms are developed to show the partition of the adsorbate molecules between the liquid and solid phases under equilibrium conditions. The knowledge of the adsorption equilibrium is needed to estimate the maximum adsorption capacity of the *I. viscosa*, as well as to characterize the molecular forces involved in the process. The Langmuir, Freundlich, Temkin, and Dubinin–Radushkevich (D–R) [22–31] isotherm models are tested to discuss the adsorption behavior.

The Langmuir model is based on the monolayer coverage of adsorbate over a homogenous adsorbent surface:

$$\frac{C_e}{q_e} = \frac{1}{bq_o} + \frac{C_e}{q_o} \quad (4)$$

where C_e (mg L^{-1}) is the equilibrium dye concentrations, q_e and q_m (mg g^{-1}) are the adsorbed amounts at equilibrium and maximal capacity, and b (L mg^{-1}) is the Langmuir constant.

The Freundlich isotherm is an empirical model valid for the description of multilayer adsorption whose logarithmic form is given by:

$$\log q_e = \log K_f + \frac{1}{n} \log C_e \quad (5)$$

K_f and n are the Freundlich constants related to the adsorption capacity and adsorption intensity, respectively.

The Temkin isotherm is based on the chemical adsorption used in many processes whose linear form is expressed by:

$$q_e = B_1 \log(A) + B_1 \log C_e \quad (6)$$

where

$$B_1 = (RT/k_i) \quad (7)$$

where A (L/g) the equilibrium binding constant, corresponding to the maximum binding energy, and B a constant related to the adsorption heat.

The D–R is also tested to evaluate the porosity and the apparent energy of the adsorption and is represented by:

$$\log q_e = \log(q_{\max}) - K_{DR}\varepsilon^2 \quad (8)$$

where ε is the Polanyi adsorption potential given by:

$$\varepsilon = RT \log\left(\frac{1}{1/C_e}\right) \quad (9)$$

The mean adsorption energy E (kJ mol⁻¹) is computed from the constant K_{D-R} using the expression [2]:

$$E = \frac{1}{(-2K_{D-R})^{\frac{1}{2}}} \quad (10)$$

K_{D-R} (mol² kJ⁻²) being the activity coefficient related to the adsorption energy. The parameters of all models are gathered in Table 4.

The separation factor is a dimensionless equilibrium parameter (R_L) expressed by [33]:

$$R_L = \frac{1}{1 + bC_0} \quad (11)$$

The R_L values calculated from (b) constant of Langmuir are gathered in Table 5 while the parameter models are reported in Table 4. It appears from the higher correlation coefficient (R^2) that the Langmuir model fits well the experimental results over the investigated concentrations range. At acidic pH, the maximum adsorption capacity (q_m) of dried *I. viscosa* is found to be 43.10 mg g⁻¹, indicating that this material is a good adsorbent in the treatment of yellow tartrazine solutions (20–200 mg L⁻¹). By contrast, the D–R isotherm model is found to be inappropriate for describing the adsorption equilibrium.

On the basis of K_{D-R} values, obtained from the D–R isotherm graph, the calculated energy E is less than 10 kJ/mol whatever the pH, indicating a physisorption in the present case. From the isotherm, the E value (0.351 kJ/mol) confirms a physical adsorption [24,25]. Since the physical adsorption is the prevailing

phenomena, this indicates the possibility of better and easy regeneration of the used material.

The factor R_L is smaller than unity over pH range (1–6), thus confirming the favorable adsorption of tartrazine dye onto *I. viscosa*.

3.6. Comparison of tartrazine uptake capacities with other adsorbents

It is instructive at this level to compare the maximum adsorption capacities of tartrazine onto *I. viscosa* with those already reported in the literature (Table 6) to assess the potential application of this material. The q_m values of the monolayer capacity obtained from the Langmuir isotherm are presented by several authors. As can be seen, the adsorption capacity of *I. viscosa* has an intermediate value, showing its good efficiency for the tartrazine adsorption. Therefore, from an adsorption mechanism viewpoint at the molecular level, the Langmuir model suggests the easy anchoring of dye to the abundant functional groups of modified *I. viscosa* with the formation of monolayer surface coverage. Moreover, the low cost, the local availability, the waste management, and the renewability aspect make *I. viscosa* competitive with other adsorbents.

3.7. Thermodynamic study

The aim of a thermodynamic study is to determine the nature of the adsorption process. The experiments were carried out in magnetically stirred thermostated cylindrical Pyrex reactor. The thermodynamic parameters ΔG° , ΔH° , and ΔS° are determined from the slope and the intercept of Eq. (12) [34] at 20, 25, 30, 40, and 50°C.

$$\ln K_c = \frac{\Delta S^\circ}{R} - \frac{\Delta H^\circ}{RT} \quad (12)$$

where K_c is the equilibrium constant calculated by the following equation:

$$K_c = \frac{C_{\text{ads}}}{C_{\text{sol}}} \quad (13)$$

C_{ads} and C_{sol} are the concentrations of dye in the solid and the bulk solution, respectively, R the universal gas constant (8.314 J mol⁻¹ K⁻¹), and T the absolute temperature (K).

Fig. 8 shows the uptake removal of tartrazine at various temperatures. The adsorption rate increases with increasing temperature, while the final removal yields are similar and exceed 93% for 80 mg L⁻¹ of dye at pH 2. Moreover, increasing the temperature is known to increase the rate of diffusion of the adsorbate

Table 4
Parameter isotherm models of tartrazine dye adsorption onto *I. viscosa*

pH	1	2	3	4	5	6
Langmuir Eq. (1)						
q_o	22.85	43.10	24.96	20.46	12.0485	5.07614
B	0.0125	0.0374	0.0121	0.0034	0.04517	0.0075
R^2	0.9913	0.955	0.9846	0.3857	0.7854	0.45
Freundlich						
$1/n$	0.6779	0.5895	0.6779	0.8533	0.7485	0.5671
K_f	0.5712	0.7146	0.5713	0.1026	0.0142	0.0009
R^2	0.9875	0.8375	0.9875	0.8984	0.7548	0.9397
Temkin						
B_1	4.4133	5.0079	5.4133	3.2172	3.1425	3.5638
$k_t \times 10^{-2}$	5.6138	4.9474	4.5768	7.7010	4.8522	6.9519
R^2	0.9674	0.9404	0.9674	0.97	0.8497	0.9170
Dubinin–Radushkevich DR						
$K_{D-R} 10^2$	-2.1344	-1.1315	-6.4402	-2.4344	-2.6526	-2.7974
q_m	9.82	14.62	10.55	6.53	5.47	3.41
E	4.4800	6.6475	2.7863	4.5319	4.3416	4.2277
R^2	0.7435	0.9123	0.828	0.9447	0.9251	0.7517

Table 5
 R_L value obtained at various pH for tartrazine removal over *I. viscosa*

pH	1	2	3	4	5	6
R_L	0.6153	0.3484	0.6230	0.8547	0.3068	0.7272

molecules across the external boundary layer. From the linear plots of $\ln(K_c)$ vs. $(1/T)$ the parameters ΔG° , ΔS° , and ΔH° can be calculated. A negative ΔG° value (Table 7) indicates a spontaneous adsorption. The positive values ΔH° and ΔS° suggest an endothermic nature of adsorption and increased randomness at the solid-solution interface during adsorption [35].

3.8. Kinetic study

The kinetic adsorption data are processed to understand the dynamics of the adsorption in terms

of rate constants and to know the rate-controlling step of the adsorption mechanism. Moreover, it is helpful for the prediction of adsorption rate to give important information for designing and modeling the processes.

The kinetic models of pseudo-first order and pseudo-second order are presented by the following equations [36]:

$$\log(q_e - q_t) = \log(q_e) - \frac{k_1}{2.303} t \quad (14)$$

$$\frac{t}{q_t} = \frac{1}{k_2 q_e^2} + \frac{t}{q_e} \quad (15)$$

where q_t and q_e (mg g^{-1}) are the adsorption capacities at time t and at equilibrium, respectively, k_1 (L min^{-1}) and k_2 ($\text{g mg}^{-1} \text{min}^{-1}$) are the first- and second-order rate constants, respectively.

The Intraparticle diffusion equation is expressed by the equation of Weber and Morris [37]:

Table 6
Adsorption capacity of various adsorbents for tartrazine dye onto *I. viscosa*

Adsorbent	Optimal dosage (g L^{-1})	Initial concentration (mg L^{-1})	Optimum pH	q_e (mg g^{-1})	Ref.
Bottom Ash	0.1	5.3436	2.0	1.00	[10,15]
De-Oiled Soya	0.05	5.3436	2.0	2.13	[10,15]
Hen feathers	0.01	5.3436	2	64.12 mg/g	[16]
Modified activated carbon	1	200	1	121.3	[36]
<i>Inula viscosa</i>	5	50	2	43.10	This work

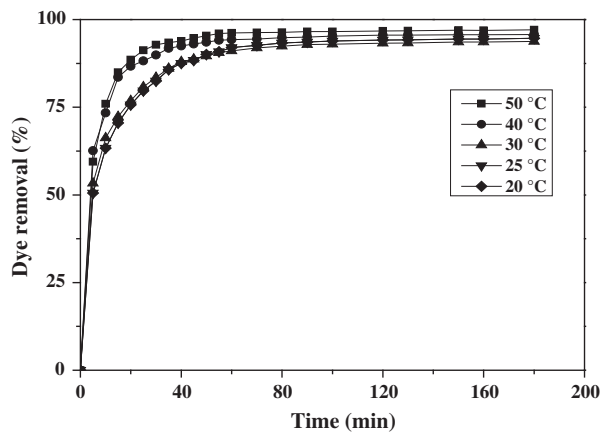


Fig. 8. Effect of the temperature on the tartrazine dye adsorption onto *I. viscosa* (80 mg L^{-1} , pH 2, 5 g L^{-1} adsorbent, 400 rpm min^{-1}).

Table 7

Thermodynamic parameters of tartrazine dye adsorption onto *I. viscosa*

Temperature (K)	ΔG (kJ mol^{-1})	ΔH ($\text{kJ mol}^{-1} \text{K}^{-1}$)	ΔS (J mol^{-1})
323	-9.6887	24.5599	105.9836
313	-8.6289		
303	-7.5690		
298	-7.0391		
293	-6.5092		

Table 8

Kinetic parameters of tartrazine dye adsorption onto *Inula viscosa*

Concentration (mg L^{-1})	20	40	50	60	80	100	150	200
q_{exp} (mg g^{-1})	3.78	7.73	9.26	9.7	15.41	16.07	18.83	25.89
Pseudo first order								
q_e (mg g^{-1})	2.41	8.87	2.93	7.94	8.73	11.34	14.48	12.091
K_1 ($\text{g mg}^{-1} \text{min}^{-1}$)	0.1083	0.0802	0.8761	0.0292	0.0742	0.0435	0.0388	0.9038
h_1 ($\text{mg g}^{-1} \text{min}^{-1}$)	0.2612	0.7109	2.5656	0.2316	0.6482	0.4927	0.5615	10.9324
R^2	0.9514	0.8968	0.7617	0.9371	0.9566	0.9617	0.8856	0.0231
Pseudo second order								
q_e (mg g^{-1})	3.9	7.88	9.61	10.54	15.93	14.19	19.75	26.54
K_2 ($\text{g mg}^{-1} \text{min}^{-1}$)	0.5403	0.1268	0.8761	0.0611	0.2244	0.1147	0.1177	1.7443
h_2 ($\text{mg g}^{-1} \text{min}^{-1}$)	2.1089	0.9995	8.4175	0.6437	3.5741	1.6287	2.3240	64.2919
R^2	0.9975	0.9963	0.999	0.9781	0.9947	0.9631	0.9833	0.9179
Intraparticle diffusion								
$K_d \cdot 10^4$ ($\text{mg g}^{-1} \text{min}^{-0.5}$)	4.4029	13.9	9.3645	5.3804	8.7992	12.8	6.6787	3.5287
R^2	0.0038	0.0424	0.0155	0.2531	0.0642	0.2256	0.1211	0.3452
Elovich								
q_e (mg g^{-1})	4.18	10.18	11.52	9.18	17.1	14.11	15.89	13.51
α ($\text{mg g}^{-1} \text{min}^{-1}$)	33.4279	4.8976	6.8449	1.9925	6.1582	3.4135	2.717	5.6956
β	2.134	0.555	0.5132	0.5081	0.3099	0.3404	0.2742	0.4068
R^2	0.8405	0.7605	0.5865	0.9825	0.8937	0.9816	0.9727	0.8695

$$q_t = k_{\text{dif}} t^{0.5} + C \quad (16)$$

where k_{dif} ($\text{mg g}^{-1} \text{min}$) is the intraparticle diffusion rate and C is the constant that gives an idea about the thickness of the boundary layer. The Elovich kinetic model can be described according to the following equation:

$$q_t = \frac{1}{\beta \ln(\alpha\beta)} + \frac{1}{\beta} \ln(t) \quad (17)$$

where α and β are the Elovich constants.

The initial adsorption rates are calculated from the pseudo-first-order and pseudo-second-order models according to the following equations:

$$h_1 = k_1 q_e^2 \quad (18)$$

$$h_2 = k_2 q_e^2 \quad (19)$$

The corresponding results are collected in Table 8. The general trend (Fig. 7(b)) is a decrease of the initial adsorption rate with increasing tartrazine concentration. This is in contradiction with the fact that q_e increases with raising C_o , thus increasing the driving force ($q_e - q_o$) for the adsorption as assumed in the derivation of the pseudo-kinetic model. Therefore, it is concluded that the initial adsorption rate is independent of the reaction, and that the pseudo-second-order model is more relevant to fit the experimental data.

It is clear from the accuracy of the model that the adsorption kinetic of tartrazine is described by the pseudo-second-order chemical reaction and that this reaction is significant in the rate-controlling step. Physical and chemical adsorptions may be indistinguishable in certain situations, and in some cases a degree of both type of bonding can be present, as with covalent bonds between two atoms having some degree of ionic character and vice versa [30,38].

4. Concluding remarks

Based on this study, a systematic investigation to determine the efficiency of extract waste (*I. viscosa*) treated by NaOH for the tartrazine removal in batch mode was undertaken. A large number of carbonyl and hydroxyl groups are observed on the surface of the activated adsorbent by FTIR analysis. The high dye removal obtained at low pHs can be attributed to an adsorption mechanism governed by electrostatic interactions between the positively charged adsorbent surface and the anionic dye species. The adsorption is found to be dependent on the initial concentration and temperature.

The equilibrium experimental data are tested to the Langmuir, Freundlich, Temkin, and Dubini-Radushkevich isotherm models. However, the Langmuir model is the most suitable for the adsorption process of tartrazine dye onto *I. viscosa*, while the kinetic data are accurately described by a pseudo-second-order kinetic model.

The thermodynamic studies show that the dye adsorption onto *I. viscosa* is spontaneous, endothermic with a low activation energy suggesting a physisorption mechanism. The large entropy clearly reveals that the adsorbent has a high affinity for the adsorption of tartrazine.

Although, a direct comparison of adsorption capacity of *I. viscosa* with other adsorbents is difficult because of non-identical experimental conditions. However, it can be observed that the adsorption capacity of *I. viscosa* for the tartrazine is reasonably good and comparable to other adsorbents.

The present study showed that the solid residue from *I. viscosa* is a promising alternative for the environmental clean-up; it can be used as an efficient adsorbent for dye removal from wastewaters and has good potential for further applications in the water treatment.

Acknowledgments

The authors gratefully acknowledge the financial support from the Faculty of Mechanical Engineering and Processes and the Faculty of Chemistry to perform this study. They also would like to express their

gratitude to Dr Dj. Miroud and Dr O. Arous for their help in SEM and FTIR analysis, respectively.

References

- [1] N.E. Llamas, M. Garrido, M.S. Di Nezio, B.S. Fernandez Band, Second order advantage in the determination of amaranth, sunset yellow FCF and tartrazine by UV-vis and multivariate curve resolution-alternating least squares. *Anal. Chim. Acta.* 655 (2009) 38–42.
- [2] V.K. Gupta, A. Mittal, D. Jhare J. Mittal, Batch and bulk removal of hazardous colouring agent Rose Bengal by adsorption techniques using bottom ash as adsorbent, *RSC Adv.* 2(22) (2012) 8381–8389.
- [3] J.H. Sun, S.P. Sun, G.L. Wang, L.P. Qiao, Degradation of azo dye Amido black 10B in aqueous solutions by Fenton oxidation process, *Dyes Pig.* 74 (2007) 647–652.
- [4] R. Lakshmipathy, N.C. Sarada, Adsorptive removal of basic cationic dyes from aqueous solution by chemically protonated watermelon (*Citrullus lanatus*) rind biomass, *Desalin. Water Treat.* (2013) 1–10. doi:10.1080/19443994.2013.812526
- [5] A. Mittal, D. Jhare, J. Mittal, Adsorption of hazardous dye Eosin Yellow from aqueous solution onto waste material De-oiled Soya: Isotherm, kinetics and bulk removal, *J. Mol. Liq.* 179 (2013) 133–140.
- [6] J. Mittal, V. Thakur, A. Mittal, Batch removal of hazardous azo dye Bismark Brown R using waste material hen feather, *Ecol. Eng.* 60 (2013) 249–253.
- [7] T. Robinson, G. McMullan, R. Marchant, P. Nigam, Remediation of dyes in textile effluent: A critical review on current treatment technologies with a proposed alternative, *Bioresour. Technol.* 77 (2001) 247–255.
- [8] M.H. Vijaykumar, P.A. Vaishampayan, Y.S. Shouche, T.B. Karegoudar, Decolourization of naphthalene-containing sulphonated azo dyes by *Kerstersia* sp. VKY1, *Enzyme and Microb. Technol.* 40 (2007) 204–211.
- [9] C.L. Mack, B. Wilhelmi, J.R. Duncan, J.E. Burgess, A kinetic study of the recovery of platinum ions from an artificial aqueous solution by immobilized *Saccharomyces cerevisiae* biomass, *Miner. Eng.* 21 (2008) 31–37.
- [10] T.H. Kim, C. Park, S. Kim, Water recycling from desalination and purification process of reactive dye manufacturing industry by combined membrane filtration, *J. Cleaner Prod.* 13 (2005) 779–786.
- [11] H. Daraei, A. Mittal, M. Noorisepehr, F. Daraei, Kinetic and equilibrium studies of adsorptive removal of phenol onto eggshell waste, *Environ. Sci. Pollut. Res.* 20 (2013) 4603–4611.
- [12] A. Mittal, V. Thakur, V. Gajbe, Adsorptive removal of toxic azo dye Amido Black 10B by hen feather, *Environ. Sci. Pollut. Res.* 20 (2013) 260–269.
- [13] B. Shi, G. Li, D. Wang, C. Feng, H. Tang, Removal of direct dyes by coagulation: The performance of preformed polymeric aluminum species, *J. Hazard. Mater.* 143 (2007) 567–574.
- [14] L.C. Morais, O.M. Freitas, E.P. Gonçalves, L.T. Vasconcelos, C.G. González Beça, Reactive dyes removal from wastewaters by adsorption on eucalyptus bark: Variables that define the process, *Water Res.* 33 (1999) 979–988. Available from: <http://www.sciencedirect.com/science/article/pii/S0043135498002942>

- [15] X. Han, W. Wang, X. Ma, Adsorption characteristics of methylene blue onto low cost biomass material lotus leaf, *Chem. Eng. J.* 171 (2011) 1–8.
- [16] A. Mittal, J. Mittal, L. Kurup, Adsorption isotherms, kinetics and column operations for the removal of hazardous dye, Tartrazine from aqueous solutions using waste materials—Bottom Ash and De-Oiled Soya, as adsorbents, *J. Hazard. Mater.* 136 (2006) 567–578.
- [17] A. Mittal, L. Kurup, J. Mittal, Freundlich and Langmuir adsorption isotherms and kinetics for the removal of tartrazine from aqueous solutions using hen feathers, *J. Hazard. Mater.* 146 (2007) 243–248.
- [18] K.N. Hong, I.C. Young, P.M. Samuel, Dye binding capacity of commercial chitin products, *J. Agri. Food. Chem.* 44 (1996) 1939–1942.
- [19] D. Prahas, Y. Kartika, N. Indraswati, S. Ismadji, Activated carbon from jackfruit peel waste by H_3PO_4 chemical activation: Pore structure and surface chemistry characterization, *Chem. Eng. J.* 140 (2008) 32–42.
- [20] P. Pengthamkeerati, T. Satapanajaru, O. Singchan, Sorption of reactive dye from aqueous solution on biomass fly ash, *J. Hazard. Mater.* 153 (2008) 1149–1156.
- [21] A.M.M. Vargas, A.L. Cazetta, M.H. Kunita, T.L. Silva, V.C. Almeida, Adsorption of methylene blue on activated carbon produced from flamboyant pods (*Delonix regia*): Study of adsorption isotherms and kinetic models, *Chem. Eng. J.* 168 (2011) 722–730.
- [22] M.M.V. Alexandro, L.C. André, C.M. Alessandro, C.G.M. Juliana, E.G. Edivaldo, F.G. Gisele, F.C. Willian, C.A. Vitor, Kinetic and equilibrium studies: Adsorption of food dyes Acid Yellow 6, Acid Yellow 23, and Acid Red, *Chem. Eng. J.* 181 (2012) 243–250.
- [23] Z.A. Zakaria, M. Suratman, N. Mohammed, W.A. Ahmad, Chromium (VI) removal from aqueous solution by untreated rubber wood sawdust, *Desalination* 244 (2009) 109–121.
- [24] N. Kannan, M.M. Sundaram, Kinetics and mechanism of removal of methylene blue by adsorption on various carbons—A comparative study, *Dyes Pigm.* 51 (2001) 25–40.
- [25] V.K. Garg, R. Gupta, A.B. Yadav, R. Kumar, Dye removal from aqueous solution by adsorption on treated sawdust, *Bioresour. Technol.* 89 (2003) 121–124.
- [26] Z. Aksu, G. Dönmez, A comparative study on the bio-sorption characteristics of some yeasts for Remazol Blue reactive dye, *Chemosphere* 50 (2003) 1075–1083.
- [27] F. Wu, R. Tseng, R. Juang, Kinetic modeling of liquid-phase adsorption of reactive dyes and metal ions on chitosan, *Water Res.* 35 (2001) 613–618.
- [28] H.W. Chung, Adsorption of reactive dye onto carbon nanotubes: Equilibrium, kinetics and thermodynamics, *J. Hazard. Mater.* 144 (2007) 93–100.
- [29] A. Olgun, N. Atar, Removal of copper and cobalt from aqueous solution onto waste containing boron impurity, *Chem. Eng. J.* 167 (2011) 140–147.
- [30] Y. Yao, B. He, F. Xu, X. Chen, Equilibrium and kinetic studies of methyl orange adsorption on multiwalled carbon nanotubes, *Chem. Eng. J.* 170 (2011) 82–89.
- [31] M.T. Sulak, H.C. Yatmaz, Removal of textile dyes from aqueous solutions with eco-friendly biosorbent, *Deslin. Water Treat.* 37 (2012) 169–177.
- [32] M.G. Zuhra, M.I. Bhangar, M. Akhtar, N.T. Farah, R.M. Jamil, Adsorption of methyl parathion pesticide from water using watermelon peels as a low cost adsorbent, *Chem. Eng. J.* 138 (2008) 616–621.
- [33] A. Tabak, N. Baltas, B. Afsin, M. Emirik, B. Caglar, E. Eren, Adsorption of Reactive Red 120 from aqueous solutions by cetylpyridinium-bentonite, *J. Chem. Technol. Biotechnol.* 85 (2010) 1199–1207.
- [34] L. Monser, N. Adhoum, Tartrazine modified activated carbon for the removal of Pb(II), Cd(II) and Cr(III), *J. Hazard. Mater.* 161 (2009) 263–269.
- [35] M. Kebir, M. Chabani, N. Nasrallah, A. Bensmaili, M. Trari, Coupling adsorption with photocatalysis process for the Cr(VI) removal, *Desalination* 270 (2011) 166–173.
- [36] M.N. Mohammad, Equilibrium, kinetics and thermodynamics of dye removal using alginate in binary systems, *J. Chem. Eng. Data.* 56 (2011) 2802–2811.
- [37] W.J. Weber, J.C. Morris, Kinetics of adsorption on carbon from solutions, *J. Sanit. Eng. Div. Am. Soc. Eng.* 89 (1963) 31–59.
- [38] E. Bulut, M. Ozacar, I.A. Sengil, Adsorption of malachite green onto bentonite: Equilibrium and kinetic studies and process design. Microporous Mesoporous Mater. 115 (2008) 234–246.